Higher Order Workshop 3: Problem C1.4
Vortex Transport by Uniform Flow

Presented by

Brian C. Vermeire
Philip Zwanenburg
Siva Nadarajah

Computational Aerodynamics Group

McGill University
Montreal, Quebec, Canada

Summary

A high-order Collocation Penalty via Reconstruction (CPR) computational fluid dynamics code that solves the compressible Euler equations equations was applied to the problem of vortex transport by a uniform flow to test the method's capability to preserve vorticity in an unsteady inviscid flow. The third-order explicit Runge-Kutta scheme of Shu and Osher [1] is used to advance the simulation in time.

1 Code Description

The conservation laws are discretized by the correction procedure via reconstruction (CPR) scheme with DG correction functions. The divergence of the inviscid fluxes are determined either through a chain rule or Lagrange polynomial approach. The Roe flux is employed as the common interface flux. The solver is parallelized using MPI via Open MPI, version *1.4.3* where grid partitioning is achieved through ParMETIS. Post-processing was performed with Tecplot 360.

1.1 Computations

The *Guillimin* cluster of the McGill high performance computing (MHPC) infrastructure, part of the Compute Canada HPC network, served for the computations, using the sw architecture. Machine specifications and Taubench results are presented in Tables 1 and 2.

Machine name	Specifications
MHPC-(sw)	Dual Intel Westmere EP Xeon X5650 (6-core, 2.66 GHz, 12MB Cache, 95W)

Table 1: Computer specifications

Machine name	Taubench CPU times
MHPC-(sw)	9.5 (s)

Table 2: Taubench results

2 Case Summary

The following two vortex flow conditions were specified with velocity and temperature perturbations given in the case description:

Slow Vortex		
$M_\infty = 0.05$	$\beta = 0.02$	$R = 0.005$

Fast Vortex		
$M_\infty = 0.5$	$\beta = 0.2$	$R = 0.005$

Time period, T	$\frac{L_x}{U_{\text{inf}}}$
Final time	$50T$

Residual tolerances or other convergence criteria:
Simulation run until 50T.

Polynomial	Mesh Size	# procs
P2	16 x 16	12
	32 x 32	24
	64 x 64	48
	128 x 128	48
P3	16 x 16	24
	32 x 32	48
	64 x 64	72
	128 x 128	96
P4	16 x 16	36
	32 x 32	60
	64 x 64	96

Table 3: Number of machines used

3 Meshes

Meshes used were quad meshes provided on the 3rd higher order workshop website. For the uniform grids, the meshes provided were used without modification. For the perturbed grids, the boundary nodes were adjusted such that the periodic nodes had the same x and y coordinates; node coordinates on the left and bottom were used to modify node coordinates on the right and top of the grid. The number of DOF/element was $(P+1)^2$.

Domain size (periodic square):
$0, 0 \leq x, y \leq L_x, L_y; L_x = L_y = 0.1$

4 Results

Only the slow vortex case was run.

4.1 Slow vortex

Time-step sensitivity studies were performed on the finest grids used for polynomial orders P2 to P4 on the uniform meshes; halving the time-step used on each resulted in a change of less than 0.016 % in all cases, running for the entire simulation time of 50 periods. As the computations to validate this time-step quickly become more expensive as the mesh is refined or polynomial order is increased, no time-step study was done for the perturbed meshes. Instead, time-step values used were half of those used for the uniform mesh. The assumption that the change in the error would remain insignificant is reliant on the fact that the perturbation of each node was less than or equal to 15 % of h.

Plots of integrated L_2 error norms for u, v and $\sqrt{u^2+v^2}$ are shown below along with tables showing convergence rates.

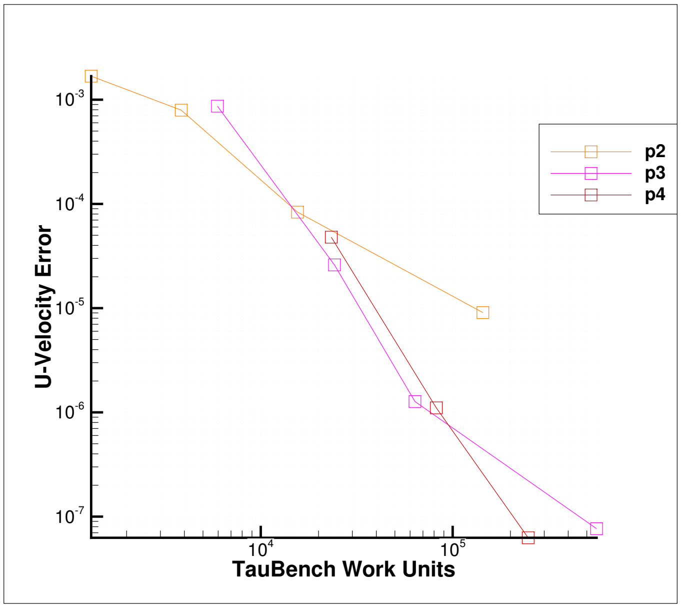

Figure 1: Integrated L_2 Norm of u-Velocity Error - Uniform Meshes

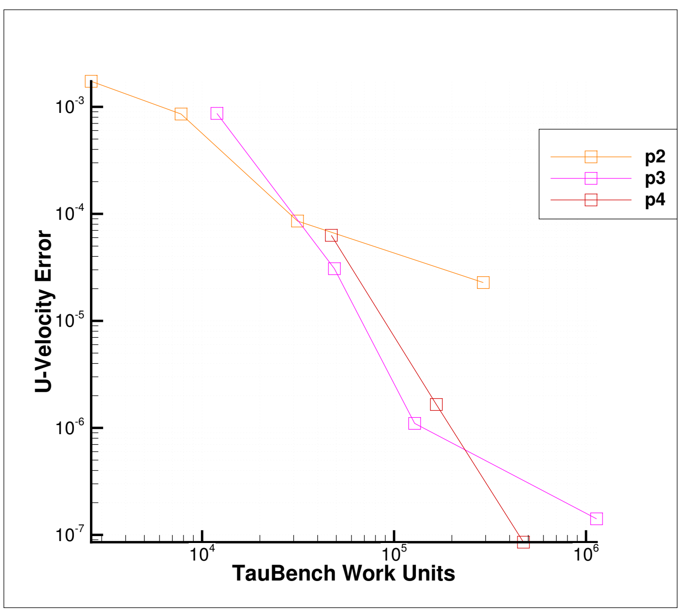

Figure 2: Integrated L_2 Norm of u-Velocity Error - Perturbed Meshes

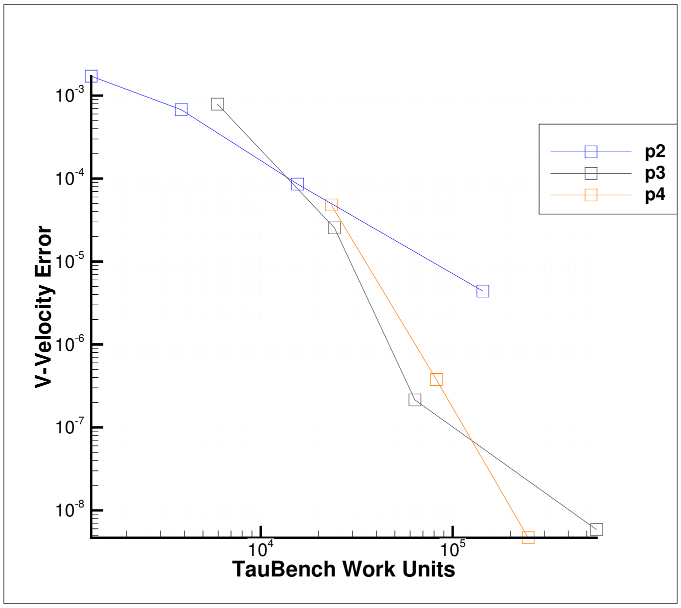

Figure 3: Integrated L_2 Norm of v-Velocity Error - Uniform Meshes

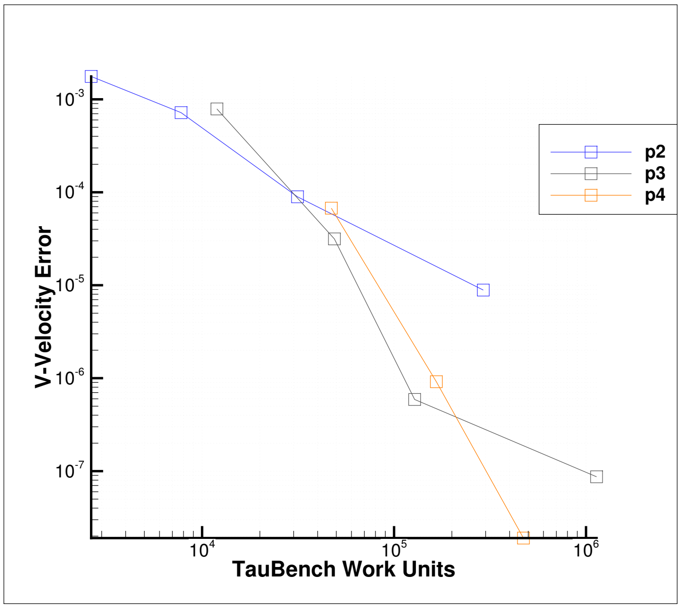

Figure 4: Integrated L_2 Norm of v-Velocity Error - Perturbed Meshes

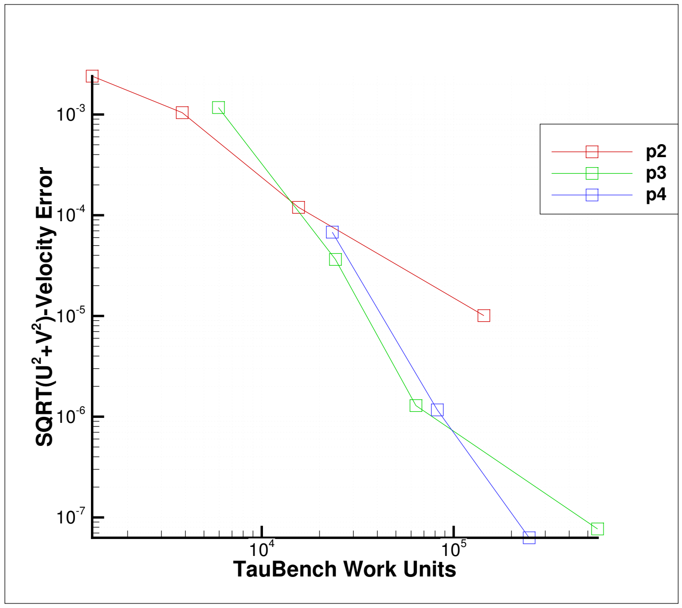

Figure 5: Integrated L_2 Norm of $\sqrt{u^2+v^2}$-Velocity Error - Uniform Meshes

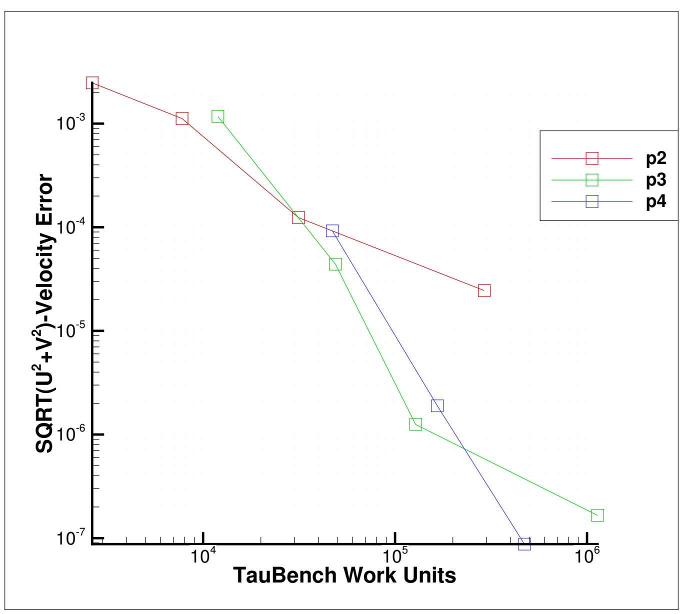

Figure 6: Integrated L_2 Norm of $\sqrt{u^2+v^2}$-Velocity Error - Perturbed Meshes

		L_2 Error			Order		
Polynomial	Mesh Size	U	V	$\sqrt{U^2+V^2}$	U	V	$\sqrt{U^2+V^2}$
P2	16 x 16	1.68e-03	1.72e-03	2.40e-03	-	-	-
	32 x 32	7.94e-04	6.76e-04	1.04e-03	1.08	1.34	1.20
	64 x 64	8.34e-05	8.58e-05	1.20e-04	3.25	2.98	3.12
	128 x 128	9.07e-06	4.40e-06	1.01e-05	3.20	4.29	3.57
P3	16 x 16	8.67e-04	7.89e-04	1.17e-03	-	-	-
	32 x 32	2.60e-05	2.55e-05	3.64e-05	5.06	4.95	5.01
	64 x 64	1.27e-06	2.14e-07	1.29e-06	4.35	6.89	4.82
	128 x 128	7.66e-08	5.87e-09	7.68e-08	4.05	5.19	4.07
P4	16 x 16	4.80e-05	4.81e-05	6.79e-05	-	-	-
	32 x 32	1.10e-06	3.78e-07	1.17e-06	5.44	6.99	5.86
	64 x 64	6.26e-08	4.68e-09	6.28e-08	4.14	6.34	4.22

Table 4: Errors and convergence orders - uniform meshes

		L_2 Error			Order		
Polynomial	Mesh Size	U	V	$\sqrt{U^2+V^2}$	U	V	$\sqrt{U^2+V^2}$
P2	16 x 16	1.73e-03	1.76e-03	2.47e-03	-	-	-
	32 x 32	8.57e-04	7.19e-04	1.12e-03	1.02	1.29	1.14
	64 x 64	8.57e-05	8.94e-05	1.24e-04	3.32	3.01	3.18
	128 x 128	2.28e-05	8.87e-06	2.45e-05	1.91	3.33	2.34
P3	16 x 16	8.68e-04	7.88e-04	1.17e-03	-	-	-
	32 x 32	3.07e-05	3.15e-05	4.40e-05	4.82	4.65	4.74
	64 x 64	1.10e-06	5.90e-07	1.25e-06	4.80	5.74	5.14
	128 x 128	1.41e-07	8.69e-08	1.66e-07	2.96	2.76	2.91
P4	16 x 16	6.30e-05	6.75e-05	9.23e-05	-	-	-
	32 x 32	1.65e-06	9.16e-07	1.89e-06	5.25	6.20	5.61
	64 x 64	8.55e-08	1.91e-08	8.76e-08	4.27	5.59	4.43

Table 5: Errors and convergence orders - perturbed meshes

References

[1] C. Shu and S. Osher. Efficient implementation of essentially non-oscillatory shock-capturing schemes. Journal of Computational Physics, 77(2):439-471, August 1988.

[2] G. Karypis and V. Kumar. A fast and high quality multilevel scheme for partitioning irregular graphs. SIAM Journal on Scientific Computing, 20(1):359-392, January 1998.

[3] B. C. Vermeire, Adaptive Implicit-Explicit Time Integration and High-Order Unstructured Methods for Implicit Large Eddy Simulation, Ph.D. Thesis, McGill University, 2014.